Article

Feasibility of a Patient-Specific Bolus Using the Life-Casting Method for Radiation Therapy

Jeongho Kim [1], Jeehoon Park [1], Beomjun Park [2,3,4], Byungdo Park [1,*,†] and Tae-Gyu Kim [1,*,†]

[1] Department of Radiation Oncology, Samsung Changwon Hospital, Sungkyunkwan University School of Medicine, Changwon 51353, Republic of Korea; jeongho5248.kim@samsung.com (J.K.); jeehoon817.park@samsung.com (J.P.)

[2] Department of Chemistry, Konkuk University, Seoul 05029, Republic of Korea; pbj0116@korea.ac.kr

[3] Advanced Crystal Material/Device Research Center, Konkuk University, Seoul 05029, Republic of Korea

[4] Interdisciplinary Program in Precision Public Health, Korea University, Seoul 02841, Republic of Korea

[*] Correspondence: byungdo.park@samsung.com (B.P.); tg1.kim@samsung.com (T.-G.K.); Tel.: +82-055-233-5668 (B.P.); +82-055-233-6085 (T.-G.K.)

[†] These authors contributed equally to this work.

Abstract: Radiation therapy for treating shallow tumors is challenging, necessitating the use of boluses. This study introduces the first application of the life-casting method to fabricate patient-specific bolus molds from gypsum sheets, comparing them with commercial boluses. Our developed boluses reduced the air gap between the skin and bolus by 77.62% compared to that of commercial boluses. In vivo dosimetry using the patient-specific bolus demonstrated better results compared to using a commercial bolus. When using the commercial bolus, the mean %Diff and max %Diff were $1.10 \pm 0.61\%$, respectively, and 2.00% for three-dimensional conformal radiation therapy (3D-CRT) and $7.19 \pm 1.90\%$ and 10.14% for volumetric modulated arc therapy (VMAT), respectively. Contrastingly, our developed bolus demonstrated more accurate dose delivery with a mean %Diff and max %Diff of $0.82 \pm 0.61\%$ and 1.69% for 3D-CRT and $3.42 \pm 1.01\%$ and 5.03% for VMAT, respectively. Furthermore, the standard deviation between the measurements was more than 50% lower when using a patient-specific bolus than when using a commercial bolus. These results show that our bolus reduces air gaps, improves the accuracy of bolus positioning, and enhances the precision of dose delivery compared with the performance of commercial boluses. Therefore, the developed bolus is expected to be valuable in clinical applications.

Keywords: life-casting; patient-specific bolus; silicone rubber; radiation therapy; air gap

1. Introduction

During radiation therapy, electron beams are predominantly utilized for the treatment of shallow tumors, such as cancers of the breast, skin, head, and neck. However, these beams are associated with the problem of inhomogeneous dose distribution, which can lead to inadequate target coverage [1,2]. Although photon beams can be employed as an alternative, the implementation of an extra material, known as a bolus, is necessary to improve the efficacy of radiation therapy, specifically to mitigate the skin-sparing effect (build-up effect) [1–4]. A bolus is utilized to augment the dose, as well as the coverage of superficial tumors [3,4]. However, the use of conventional boluses is associated with several challenges in radiation therapy. Most boluses possess a flaky structure that fails to establish an adequate conformal contact with irregular skin surfaces, such as those of the ear, nose, and scalp of the patient [1]. Consequently, this can result in the formation of air gaps between the bolus material and an uneven skin surface [5]. These air gaps lead to a decrease in the dose coverage and dose homogeneity of the planning target volume (PTV) [1,3,6–9].

Three-dimensional (3D) printing technology facilitates the production of diverse geometries. Currently, 3D printing is used in various medical fields, including patient-specific implants and external prostheses [9]. Moreover, 3D printing technology has been effectively utilized to produce patient-specific boluses for radiation therapy [1,3,7,9,10]. Compared with conventional boluses, 3D-printed boluses have a good ability to closely conform to a patient's skin surface. Patient-specific boluses produced through 3D printing have demonstrated excellent efficacy in radiotherapy because they closely adhere to the skin. However, their practical application has been hindered by certain limitations, such as the immaturity of printed materials, inconvenience, time-consuming preparation, and additional dosing [3]. Moreover, they require costly supplementary equipment, including 3D printers and accessories, which limit their clinical applicability.

Recently, devices capable of simultaneously performing dose measurements and bolus effects using gel dosimeters have been developed. Sheykholeslami et al. developed and evaluated a dual-application polyvinyl alcohol glutaraldehyde methyl thymol blue Fricke hydrogel (PVA-GTA-MTB) gel dosimeter. The PVA-GTA-MTB gel dosimeter can be easily fabricated, is suitable for dose assessment, is minimally toxic, and has a smaller air gap than does the SuperFlab bolus. This can be highly beneficial in clinical settings. However, this study did not conduct airgap quantification, and it appears that airgap issues still persist in clinical practice [11]. Furthermore, in gel dosimetry, the density can change during radiation exposure, and such changes are likely to occur with each fraction of the radiation treatment [12]. This could potentially lead to alterations in the delivered dose within a specific range.

The life-casting (LC) method is a technique that allows for the direct utilization of a living body as the primary model. LC refers to the 3D portrayal technology of a living object using casting materials and techniques [13]. In the present study, we developed bolus molds using easily accessible and cost-effective gypsum sheets and employed the LC method for their fabrication. Subsequently, we assessed the performance of the patient-specific boluses produced using these molds.

2. Materials and Methods

2.1. Fabrication of a Patient-Specific Bolus Using the LC Method

Figure 1 shows the fabrication procedure for a patient-specific bolus constructed using the LC method for the breast region. The bolus material used was EcoFlex^{TM} 0020 (Durometer Shore 0.2), which is a silicone rubber compound supplied by Smooth-On, EcoFlex^{TM} 0020. It is composed of a resin and curing agent with a mixing ratio of 1:1. The curing time is 4 h, and the shrinkage ratio is less than 0.001. EcoFlex^{TM} 0020 exhibits advantageous characteristics for casting, including ease of mold filling, flexibility, and slight tackiness.

Moreover, its density is similar to that of water [14]. The mass density and effective atomic number of EcoFlex^{TM} are 1.07 g/cm^3 and 11.66, respectively. The elemental composition (atomic weight, %) of EcoFlex^{TM} 0020 is as follows: H (7.3), C (28.9), O (4.7), Na (0.2), and Si (58.9) [15,16]. In the study by Wang et al., dosimetric tests were conducted using the EcoFlex^{TM} 0020. According to their results, the depth of the maximum dose was sufficiently similar to that of water. The percent depth dose (PDD) graph input into the treatment planning system (TPS) is measured in water. For materials similar to water, it is straightforward to determine the depth of the maximum dose based on the thickness [14]. Silicone rubber has demonstrated biocompatibility in bolus applications and has been utilized in various instances within this field [14–20]. EcoFlex^{TM} 0020 is marketed by the vendor as a "skin-safe" product [14]. The 3D printing method requires acquiring computed tomography (CT) scans of the patient or phantom, importing the CT images into a TPS to generate the bolus structure, converting the structure into an STL file, and performing the postprocessing procedures [21]. This procedure, along with the mold printing, is time-intensive. Furthermore, owing to the need for CT scans using the fabricated bolus, there is an increase in the exposure to radiation. In this study, the LC method was employed,

which enabled a considerably more streamlined fabrication of the bolus compared with the currently available 3D printing techniques.
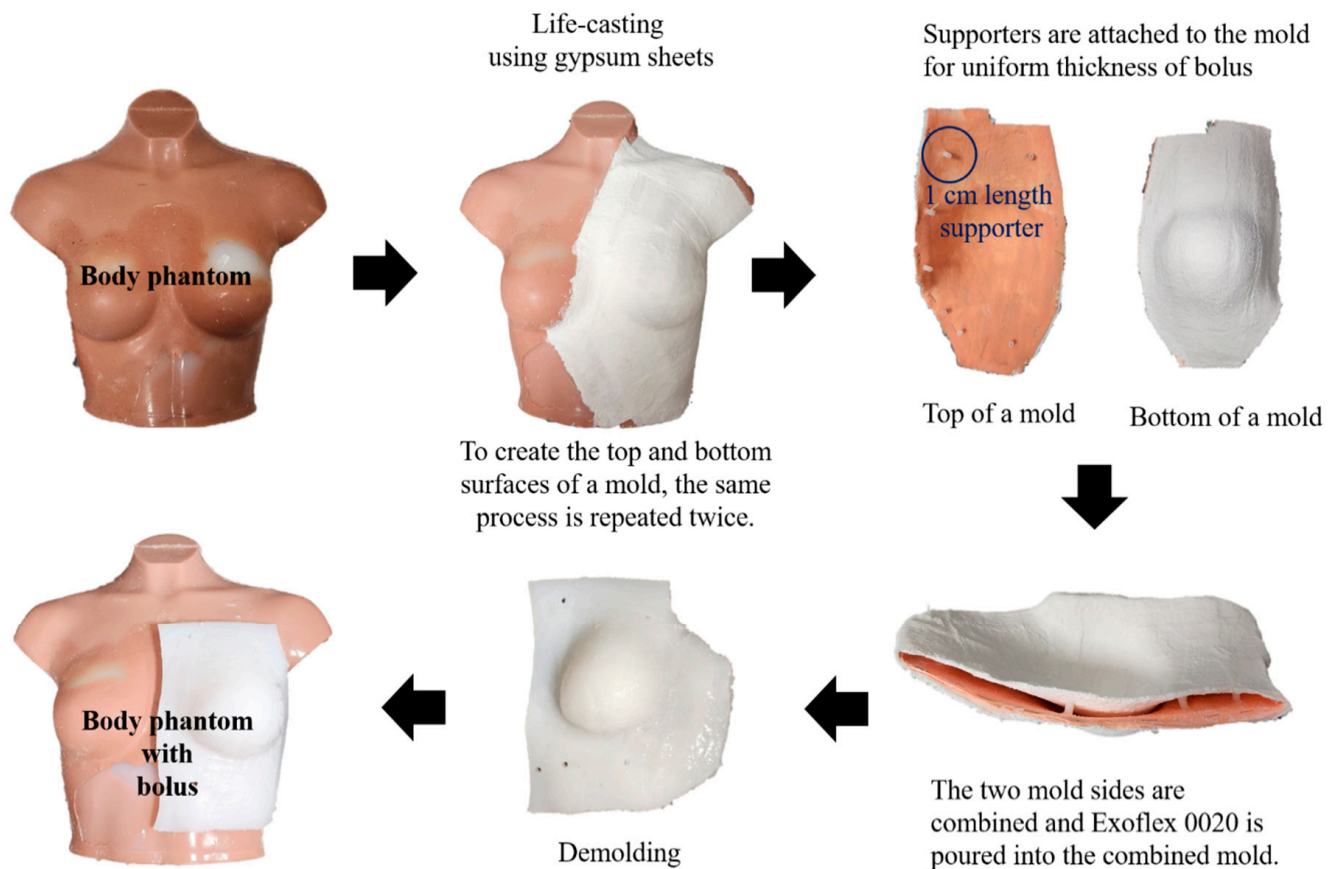

Figure 1. Fabrication procedure for a patient-specific bolus using the life-casting (LC) method.

The fabrication procedure is illustrated in Figure 1. First, wet Nok-San Cast gypsum sheets (Nok-San, Seoul, Republic of Korea) were affixed to an in-house phantom or to the patient's skin. The tissues, bones, and lungs in the in-house phantom were simulated using silicone rubber (EcoFlex^{TM} 0020), gypsum sheets (Nok-San Cast), and air, respectively. Once dried, rapid-curing silicone rubber was applied, and another gypsum sheet was attached to the top and bottom of the mold. To prevent distortion of both surfaces, holes were introduced, and support rods were used for stabilization. Subsequently, a support layer with the desired thickness was applied between the two surfaces. The support layer was fabricated using acrylic, and the thickness of the support layer was 1 cm. The surfaces were then covered with gypsum sheets, excluding the area designated as EcoFlex^{TM} 0020. Demolding was performed after pouring and curing with EcoFlex^{TM} 0020.

2.2. Air-Gap Quantification

Figure 2 shows the patient-specific bolus produced using the LC method and the commercially available SuperFlab bolus (Radiation Products Design Inc., Albertville, MN, USA) attached to the in-house phantom. To assess the conformity of the patient-specific bolus to the patient's skin surface and the presence of an air gap between the bolus and skin, CT scans were conducted with both the SuperFlab bolus and the patient-specific bolus attached to the in-house phantoms. For the SuperFlab bolus and patient-specific bolus trials, radiation therapists optimized the air gaps to the best of their abilities by following the standard protocol at our institute, where the testing was conducted. CT was performed using a Discovery CT590 RT simulator (GE Healthcare, Milwaukee, WI, USA). All the reconstructed CT images had a slice thickness of 2.5 mm. the air-gap volumes were analyzed using the CT images.
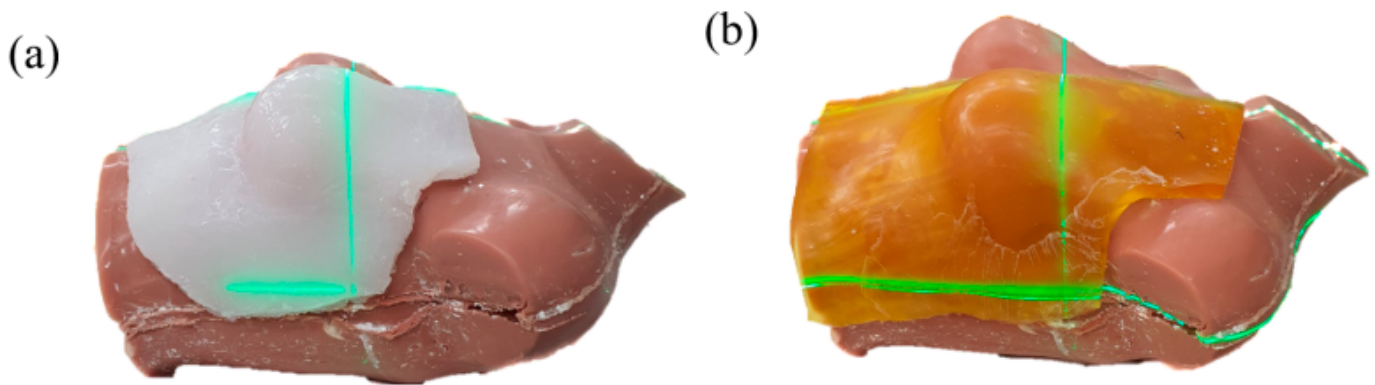
Figure 2. In-house phantom with (**a**) patient-specific bolus and (**b**) SuperFlab bolus.

2.3. Treatment Planning

Treatment plans were used to assess the impact of the patient-specific boluses on dose distribution. We developed 3D conformal radiation therapy (3D-CRT) and volumetric modulated arc therapy (VMAT) treatment plans for each bolus. All treatment plans were created for the in-house phantom using Eclipse Treatment Planning System version 16 (Varian Medical System, Palo Alto, CA, USA). The anisotropic analytical algorithm and the photon optimizer algorithm were used for all plans. For 3D-CRT, two treatment plans were formulated for the in-house phantom using a SuperFlab bolus or patient-specific bolus. In all 3D-CRT plans, parallel-opposed tangential fields were employed using a 6 MV photon beam. The maximum dose rate was set at 600 monitor units per minute (MU/min), and a 10° dynamic wedge filter was used. To assess the clinical feasibility of patient-specific boluses using the LC method in complex radiotherapy scenarios, two VMAT plans were generated, one with a SuperFlab bolus, and the other with a patient-specific bolus. A 6 MV flattening filter-free photon beam was used, with rotating gantry angles of 300° to 179° (four arcs). The maximum administered dose was 600 MU/min. The prescription dose for the PTV in all plans was 50 Gy in 25 fractions.

2.4. Dosimetric Evaluation

All treatment plans were analyzed and compared using dose-volume histograms (DVHs). The quality of the plans was evaluated based on the dosimetric parameters for the target and sparing of the left lung and heart tissues. The dosimetric parameters for the target were the $V_{95\%}$ (target coverage), the conformity index (CI), and the homogeneity index (HI). The CI is a metric used to determine how tightly the prescription dose conforms to the target and is calculated as follows:

$$CI = \frac{TV_{PIV} \times TV_{PIV}}{TV \times V_{RI}}$$

where V_{PIV} is the target volume enclosed by the reference isodose, TV is the target volume, and V_{RI} is the reference isodose volume. HI refers to the uniformity of dose distribution within the target volume and is determined as follows:

$$HI = \frac{D_{2\%} - D_{98\%}}{D_{50\%}}$$

where $D_{2\%}$ is the near-maximal dose, $D_{98\%}$ is the near-minimal dose, and $D_{50\%}$ is the median dose [22]. For the lung, we analyzed the V_{20Gy} and mean dose, and for the heart, we analyzed the V_{25Gy} and mean dose.

2.5. In Vivo Dosimetry Using Optically Stimulated Luminescence Dosimetry (OSLD)

All treatments were conducted using the TrueBeam STx (Varian Medical Systems, Palo Alto, CA, USA). Figure 3 illustrates in vivo dosimetry using OSLD (InLight®nanoDot™, Landauer, IL, USA). To evaluate the suitability and reproducibility of the bolus, in vivo dosimetry was conducted by performing three measurements at four points for each plan, with the bolus applied. The differences between the calculated and measured doses at these four points were determined to investigate the uncertainty of the bolus structures. The percentage difference (%Diff) was calculated as follows [23]:

$$\%\text{Diff} = \frac{\text{Measured dose} - \text{Calculated dose}}{\text{Calculated dose}} \times 100$$
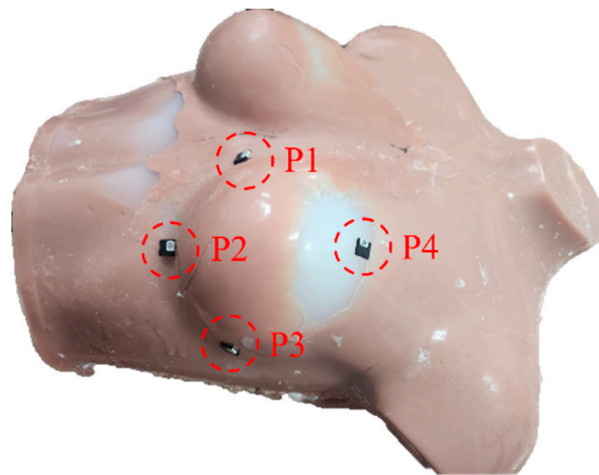

Figure 3. Optically stimulated luminescent dosimetry (OSLD) measurement points for in vivo dosimetry.

3. Results

3.1. Air Gap Quantification

Figure 4 shows the air gaps between the skin surface and each bolus. In the case of curved surfaces, the patient-specific bolus fabricated using the LC method demonstrated a reduction in the air gap between the skin surface and bolus compared to the SuperFlab bolus. When utilizing the patient-specific bolus fabricated in this study, the total air-gap volume was measured as 9.51 cm^3, whereas the SuperFlab bolus yielded a volume of 42.5 cm^3. These findings demonstrate a substantial 77.62% reduction in the total air gap when using the patient-specific bolus compared to the commercially available alternative.

3.2. Dosimetric Evaluation

Figure 5 and Table 1 present the DVH and dosimetric results for each plan, respectively. The DVH demonstrated small variations in the dosimetric results between the two types of boluses. Both 3D-CRT plans exhibited the same target conformity, whereas the use of a patient-specific bolus improved the homogeneity and target coverage. Regarding organ-at-risk (OAR) sparing, the delivery of radiation doses to the lungs and heart was higher when using a patient-specific bolus. However, both plans met the dose constraints, with the parameters of the lung $V_{20\text{Gy}} < 30\%$ and the mean lung dose < 17 Gy being satisfied for both plans, as well as the $V_{25\text{Gy}} < 10\%$ and the mean dose < 15 Gy for the heart.
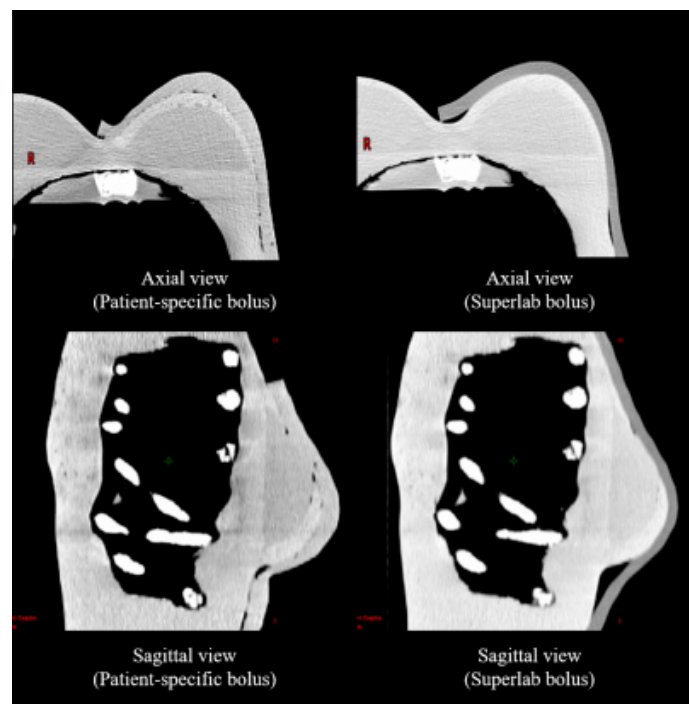
Figure 4. Axial and sagittal views of the phantom's computed tomography (CT) image using the patient-specific bolus and the SuperFlab bolus.

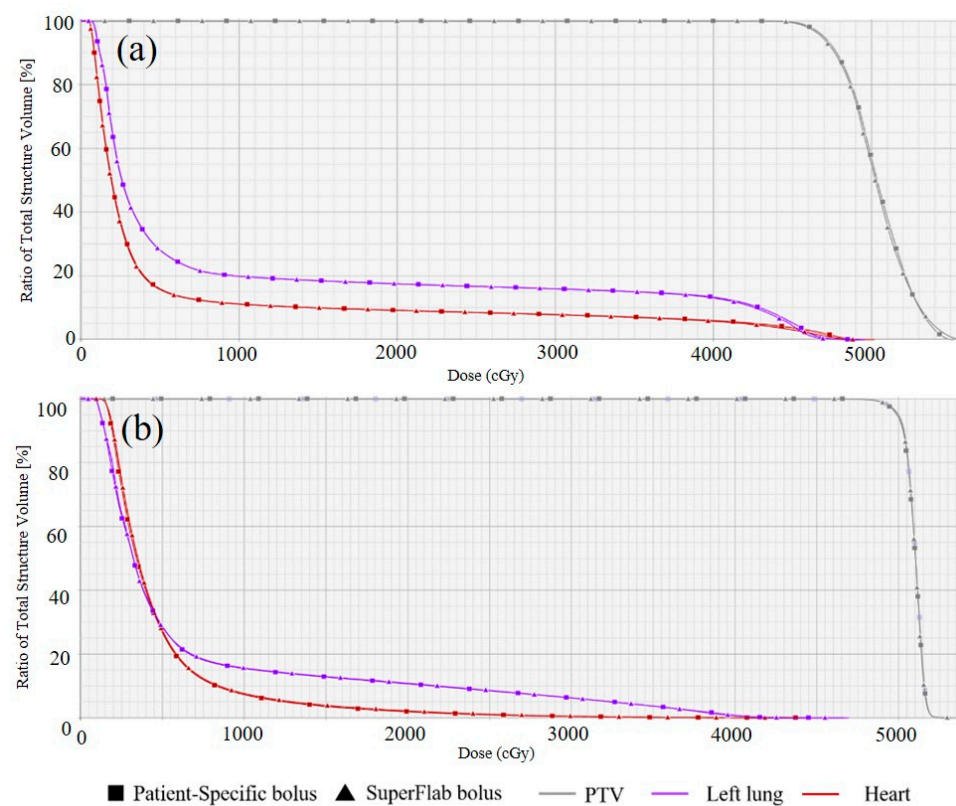**Figure 5.** Dose-volume histogram (DVH) of (**a**) three-dimensional conformal radiation therapy (3D-CRT) plans and (**b**) volumetric modulated arc therapy (VMAT) plans with the patient-specific bolus and the SuperFlab bolus.

Table 1. Dosimetric results for each plan.

Dosimetric Parameter	3D-CRT		VMAT	
	Patient-Specific Bolus	SuperFlab Bolus	Patient-Specific Bolus	SuperFlab Bolus
CI_PTV	0.31	0.31	0.94	0.93
HI_PTV	0.16	0.17	0.05	0.05
$V_{95\%}$_PTV (%)	92.2	91.3	100.0	99.8
V_{20Gy}_Lung (%)	17.5	17.5	10.8	10.7
D_{mean}_Lung (Gy)	9.72	9.66	6.84	6.79
V_{25Gy}_Heart (%)	8.50	8.45	1.13	0.97
D_{mean}_Heart (Gy)	5.92	5.82	4.84	4.71

Abbreviations: 3D-CRT, three-dimensional conformal radiation therapy; VMAT, volumetric modulated arc therapy; CI, conformity index; PTV, planning target volume; $V_{95\%}$, target coverage; HI, homogeneity index.

In the VMAT plan, both boluses exhibited the same target homogeneity, whereas the use of a patient-specific bolus improved the conformity and target coverage. For the OAR, higher doses were delivered using the patient-specific bolus. However, both plans met the dose constraints and satisfied the parameters of the lung at $V_{20Gy} < 30\%$ and the mean lung dose < 17 Gy, and a $V_{25Gy} < 10\%$ and the mean dose < 15 Gy for the heart.

3.3. In Vivo Dosimetry Using OSLD

Table 2 displays the expected dose values in the treatment plan, the dose values measured using OSLD, and the %Diff between the two values. To minimize the setup errors introduced by the operator, the setup for all tests in this study was conducted using the ExacTracDynamic® system version 1.0 (Brainlab AG, Munich, Germany), a surface guided radiation therapy system. In the 3D-CRT plan, the patient-specific bolus showed a mean %Diff of $0.82 \pm 0.61\%$ and a maximum %Diff of 1.69%. In contrast, when the SuperFlab bolus was used, the mean %Diff was measured as $1.10 \pm 0.61\%$, while the maximum %Diff was 2.00%. It is worth noting that the analysis of the three measurements for each point revealed a higher maximum standard deviation between the measurements obtained with the SuperFlab bolus (7 cGy) than with the patient-specific bolus (3 cGy).

Table 2. In vivo dosimetry results for each plan.

3D-CRT							
Patient-Specific Bolus				SuperFlab Bolus			
Point	Plan (cGy)	OSLD (cGy, Mean ± SD)	%Diff (%)	Point	Plan (cGy)	OSLD (cGy, Mean ± SD)	%Diff (%)
P1	189	189 ± 1	0.31	P1	194	192	0.88
P2	202	206 ± 3	1.69	P2	209	213 ± 7	2.00
P3	202	202 ± 1	0.20	P3	198	201 ± 2	1.19
P4	204	206 ± 2	1.08	P4	203	202 ± 4	0.32
VMAT							
Patient-Specific Bolus				SuperFlab Bolus			
Point	Plan (cGy)	OSLD (cGy, Mean ± SD)	%Diff (%)	Point	Plan (cGy)	OSLD (cGy, Mean ± SD)	%Diff (%)
P1	148	144 ± 7	2.33	P1	145	138 ± 9	4.85
P2	50	52 ± 8	2.86	P2	51	56 ± 14	10.1
P3	188	181 ± 5	3.46	P3	180	192 ± 5	6.83
P4	195	185 ± 4	5.03	P4	185	172 ± 7	6.94

Abbreviations: OSLD, optically stimulated luminescence dosimetry; SD, standard deviation; 3D-CRT, three-dimensional conformal radiation therapy; VMAT, volumetric modulated arc therapy.

In the VMAT plan, utilizing the patient-specific bolus resulted in a mean %Diff of $3.42 \pm 1.01\%$. Conversely, employing the SuperFlab bolus yielded a higher mean %Diff of $7.19 \pm 1.90\%$. The maximum %Diff observed for the patient-specific bolus was 5.03%, whereas the maximum %Diff observed for the SuperFlab bolus was 10.1%. Moreover, considering the results of the three measurements, the maximum standard deviation between the measurements was higher with the SuperFlab bolus (14 cGy) than with the patient-specific bolus (8 cGy).

4. Discussion

In this study, we developed a patient-specific bolus by using the LC method and compared it with a commercial bolus. When comparing the dosimetric results of the 3DCRT and VMAT treatment plans, it was observed that using the patient-specific bolus resulted in better target coverage than using the commercial bolus. However, the doses delivered to the lung and heart were higher for both types of treatment plans when patient-specific boluses were used. Nevertheless, all the plans in this study satisfied the set dose constraints. We observed a reduction in the air gap when using a patient-specific bolus, which led to an improvement in the accuracy of the dose delivery. In particular, the commercial bolus exhibited a poorer accuracy of dose delivery in areas with a large air gap than the patient-specific bolus developed in this study. This may be attributed to the challenge of using the commercial bolus in inter-fraction setup variations. In contrast, the position of the patient-specific bolus can be consistently reproduced, even in the presence of an air gap, which can reduce the inter-fraction setup variations. This can be inferred from the lower standard deviation observed in the measured values when a patient-specific bolus was used for the three measurements. Furthermore, inaccuracies in the dose delivery were more pronounced in the VMAT plan, which is inherently more complex than the 3D-CRT plan.

In the study by Wang et al., 3D printing technology was employed to fabricate 3D custom boluses, which were then compared with the commercial boluses. Wang et al. reported that during treatment, patients showed a reduced air gap volume of 46.1 cm^3 when using a 3D-printed custom bolus compared to the air gap volume of 169 cm^3 exhibited by a standard bolus [14]. These findings demonstrate a substantial reduction of 72.72% in the total air gap when utilizing the 3D-printed custom bolus compared to the standard bolus. Our study results demonstrated a 77.62% reduction in the air gap when utilizing the patient-specific bolus developed in this study compared to the commercially available bolus. This finding indicates that the bolus developed in this study exhibits a performance similar to that of a bolus fabricated using 3D printing technology. Wang et al. also reported the in-vivo dosimetry results, according to which the mean absolute difference between the expected and received doses was $5.69 \pm 4.56\%$ (with a maximum of 15.1%) for the standard bolus and $1.91 \pm 1.31\%$ (with a maximum of 3.51%) for the custom bolus. In addition, another study reported that areas with larger air gaps corresponded to larger differences in the dose [14]. This finding is consistent with the results of our study and confirms that the bolus developed in our study exhibits a performance similar to that of the bolus fabricated using 3D printing technology. Furthermore, we observed certain advantages over the 3D printing technology in terms of the fabrication of the bolus. Wang et al. revealed that designing the boluses for the patient and the phantom took approximately 1 h each. Additionally, the printing of the bolus molds for the phantom and patient required approximately 2 days and 6 days, respectively. In our study, the entire process, including mold and bolus fabrication, took less than 1 day to complete. Furthermore, our study benefits from the absence of a 3D printer, which eliminates the cost and space constraints. Moreover, creating a bolus mold using a 3D printer requires a patient's CT scan; after fabrication, applying the bolus necessitates another CT scan, resulting in a total of two CT scans. This results in unnecessary radiation exposure. The method employed in the present study has the advantage of avoiding unnecessary radiation exposure.

Park et al. conducted a study on six patients who underwent post-total mastectomy radiation treatment. The 3D-printed boluses were fabricated, clinically applied, and compared with the commercial boluses [24]. Their findings showed that the commercial boluses were associated with an improvement in the dosimetric results for the target, while reducing the radiation dose delivered to the lungs and heart [24]. When compared with the results of our study, a disparity in the observed trends for OAR sparing was noted. This can be attributed to the use of a phantom rather than human participants in our study, as well as to the smaller number of treatment plans employed. Furthermore, Park et al. reported improved OAR-sparing results, albeit with differences of less than 1 Gy across all outcomes. In our study, when a patient-specific bolus was used, there was an increase in the radiation dose delivered to the OARs. However, these differences were within the range of 1 Gy or 1%. In addition, the established dose constraints were satisfied in all plans in which patient-specific boluses were employed.

These limitations can be addressed by conducting phantom studies on diverse anatomical sites before clinical implementation. In the study by Park et al., a radiochromic film was used to evaluate the accuracy of the delivered dose for each bolus. Their results indicated that the 3D-printed bolus had more precise dose delivery and smaller measurement deviations. The bolus developed in our study exhibited a similar performance to those of boluses fabricated using 3D printing technology.

Sheykholeslami et al. developed and assessed a device for simultaneous dose measurement and bolus effects using a PVA-GTA-MTB gel dosimeter. When comparing the EBT film and PVA-GTA-MTB gel dosimeters for dose assessment, Sheykholeslami et al. reported a relative difference of 4.18% in the lateral part of the breast [11]. In our study, when we compared the point dose from the TPS rather than from the EBT film, we observed a similar maximum difference of 5.08% for VMAT. One of the objectives of bolus development is to reduce the air gap between the skin and bolus. In our study, we quantified the air gap, whereas in the study by Sheykholeslami et al., no air gap quantification was performed. Moreover, in the study by Sheykholeslami et al., on examining the CT image, it appears that the air gap issue still persists. As radiation therapy often involves fractionated treatments, reproducibility is crucial for each treatment. Gel dosimetry is based on the principle that the density changes during radiation exposure, enabling the measurement of dose variations [12]. As a result, as the number of treatments increases, such variations accumulate, potentially leading to discrepancies in the initial treatment planning. The use of a new bolus for each treatment can also increase the cost-related concerns. Sheykholeslami et al. reported negligible toxicity in their study. However, if used on the skin, tests related to skin stability, such as skin sensitization and in vitro cytotoxicity, should be performed. Regarding Ecoflex^{TM}, this product has obtained skin safety certifications for all such tests [16]. Furthermore, Ecoflex^{TM} has a density of 1.07 g/cm^3, similar to that of water. In a study by Son et al. [16], when comparing the PDD values for 6 MV, the surface doses for water and Ecoflex were reported to be 98.4% and 98.6%, respectively, whereas the D10cm values were 66.6% and 66.1%, respectively, indicating that they had similar values. These characteristics are highly beneficial for clinical applications.

A limitation of our study was the difficulty in achieving a consistent thickness of the fabricated bolus. It was observed that certain parts of the bolus were thinner than desired (Figure 4). We believe that this problem can be addressed by devising a method to securely fasten the bolus material to the support structure, thereby ensuring a precise and uniform thickness.

Nevertheless, the patient-specific bolus exhibited a reduced air gap and enhanced accuracy in dose delivery compared to the commercial bolus used in the present study. In addition, the LC method employed in this study offers advantages over the 3D printing method in terms of the ease of fabrication, cost-effectiveness, and the absence of additional radiation requirements.

5. Conclusions

We applied the LC method for the first time to fabricate patient-specific boluses and evaluated their performance. Compared to commercial boluses, the LC method allowed for a reduction in the air gap, increased the accuracy of dose delivery, and improved the reproducibility of the bolus setup. In addition, the patient-specific boluses created using the LC method exhibited a similar performance to that of boluses fabricated in other studies using 3D printing techniques. This suggests that patient-specific boluses can be produced without the existing limitations, such as the cost of purchasing 3D printing and design software, spatial constraints, and long production times. In particular, the LC method offers high accessibility, as it does not require advanced 3D design skills and employs easily obtainable materials, such as plaster. Furthermore, this approach prevents unnecessary radiation exposure for the patients by reducing the number of CT scans required. Therefore, the method proposed in this study is expected to be useful for creating patient-specific boluses for radiation therapy applications.

Author Contributions: Conceptualization: J.K., T.-G.K. and B.P. (Byungdo Park); methodology: J.K.; validation: B.P. (Beomjun Park); formal analysis: J.K. and B.P. (Beomjun Park); writing—original draft preparation: J.K.; writing—review and editing: J.P., B.P. (Beomjun Park), T.-G.K. and B.P. (Byungdo Park); supervision: T.-G.K. and B.P. (Byungdo Park). All authors have read and agreed to the published version of the manuscript.

Institutional Review Board Statement: Not applicable.

Informed Consent Statement: Not applicable.

Data Availability Statement: Not applicable.

Conflicts of Interest: The authors declare no conflict of interest.

References

1. Lu, Y.; Song, J.; Yao, X.; An, M.; Shi, Q.; Huang, X. 3D printing polymer-based bolus used for radiotherapy. *Int. J. Bioprint.* **2021**, *7*, 414. [CrossRef] [PubMed]
2. Hodapp, N. The ICRU Report 83: Prescribing, recording and reporting photon-beam intensity-modulated radiation therapy (IMRT). *Strahlenther. Onkol.* **2012**, *188*, 97–99. [CrossRef] [PubMed]
3. Dipasquale, G.; Poirier, A.; Sprunger, Y.; Uiterwijk, J.W.E.; Miralbell, R. Improving 3D-printing of megavoltage X-rays radiotherapy bolus with surface scanner. *Radiat. Oncol.* **2018**, *13*, 203. [CrossRef]
4. Vyas, V.; Palmer, L.; Mudge, R.; Jiang, R.; Fleck, A.; Schaly, B.; Osei, E.; Charland, P. On bolus for megavoltage photon and electron radiation therapy. *Med. Dosim.* **2013**, *38*, 268–273. [CrossRef]
5. Aras, S.; Tanzer, İ.O.; İkizceli, T. Dosimetric comparison of superflab and specially prepared bolus materials used in radiotherapy practice. *Eur. J. Breast Health* **2020**, *16*, 167–170. [CrossRef]
6. Khan, Y.; Villarreal-Barajas, J.E.; Udowicz, M.; Sinha, R.; Muhammad, W.; Abbasi, A.N.; Hussain, A. Clinical and dosimetric implications of air gaps between bolus and skin surface during radiation therapy. *J. Cancer Ther.* **2013**, *4*, 1251–1255. [CrossRef]
7. Fujimoto, K.; Shiinoki, T.; Yuasa, Y.; Hanazawa, H.; Shibuya, K. Efficacy of patient-specific bolus created using three-dimensional printing technique in photon radiotherapy. *Phys. Med.* **2017**, *38*, 1–9. [CrossRef] [PubMed]
8. Butson, M.J.; Cheung, T.; Yu, P.; Metcalfe, P. Effects on skin dose from unwanted air gaps under bolus in photon beam radiotherapy. *Radiat. Meas.* **2000**, *32*, 201–204. [CrossRef]
9. Jreije, A.; Keshelava, L.; Ilickas, M.; Laurikaitiene, J.; Urbonavicius, B.G.; Adliene, D. Development of patient specific conformal 3D-printed devices for dose verification in radiotherapy. *Appl. Sci.* **2021**, *11*, 8657. [CrossRef]
10. Asfia, A.; Novak, J.I.; Mohammed, M.I.; Rolfe, B.; Kron, T. A review of 3D printed patient specific immobilisation devices in radiotherapy. *Phys. Imaging Radiat. Oncol.* **2020**, *13*, 30–35. [CrossRef]
11. Sheykholeslami, N.; Parwaie, W.; Vaezzadeh, V.; Babaie, M.; Farzin, M.; Geraily, G.; Karimi, A.H. Dual application of polyvinyl alcohol glutaraldehyde methylthymol blue Fricke hydrogel in clinical practice: Surface dosimeter and bolus. *Appl. Radiat. Isot.* **2023**, *197*, 110827. [CrossRef] [PubMed]
12. Hilts, M.; Jirasek, A.; Duzenli, C. Effects of gel composition on the radiation induced density change in PAG polymer gel dosimeters: A model and experimental investigations. *Phys. Med. Biol.* **2004**, *49*, 2477–2490. [CrossRef] [PubMed]
13. Derda, A.; Nadolski, M.; Muskala, K. Lifecasitng in artistic casting. *Metall. Foundry Eng.* **2011**, *11*, 63–72. [CrossRef]

14. Wang, K.M.; Rickards, A.J.; Bingham, T.; Tward, J.D.; Price, R.G. Technical note: Evaluation of a silicone-based custom bolus for radiation therapy of a superficial pelvic tumor. *J. Appl. Clin. Med. Phys.* **2022**, *23*, e13538. [CrossRef]

15. Shin, W.G.; Lee, S.Y.; Jin, H.; Kim, J.; Kang, S.; Kim, J.I.; Jung, S. Development and evaluation of a thimble-like head bolus shield for hemi-body electron beam irradiation technique. *J. Radiat. Prot. Res.* **2022**, *47*, 152–157. [CrossRef]

16. Son, J.; Jung, S.; Park, J.M.; Wu, H.G.; Kim, J.I. Evaluation of platinum-catalyzed silicones for fabrication of biocompatible patient-specific elastic bolus. 2020. *Preprint (Version 1).* Available online: https://www.researchsquare.com/article/rs-48004/v1 (accessed on 1 September 2023).

17. Kim, S.W.; Shin, H.J.; Kay, C.S.; Son, S.H. A customized bolus produced using a 3-dimensional printer for radiotherapy. *PLoS ONE* **2014**, *9*, e110746. [CrossRef]

18. Lukowiak, M.; Boehlke, M.; Lewocki, M.; Kot, W.; Matias, D.; Piątek- Hnat, M.; El Fray, M.; Jezierska, K.; Podraza, W. Use of a 3D printer to create a bolus for patients undergoing tele-radiotherapy. *Int. J. Radiat. Res.* **2016**, *14*, 287–295. [CrossRef]

19. Canters, R.A.; Lips, I.M.; Wendling, M.; Kusters, M.; van Zeeland, M.; Gerritsen, R.M.; Poortmans, P.; Verhoef, C.G. Clinical implementation of 3D printing in the construction of patient specific bolus for electron beam radiotherapy for non-melanoma skin cancer. *Radiother. Oncol.* **2016**, *121*, 148–153. [CrossRef] [PubMed]

20. Chiu, T.; Tan, J.; Brenner, M.; Gu, X.; Yang, M.; Westover, K.; Strom, T.; Sher, D.; Jiang, S.; Zhao, B. Three-dimensional printer aided casting of soft, custom silicone boluses (SCSBs) for head and neck radiation therapy. *Pract. Radiat. Oncol.* **2018**, *8*, e167–e174. [CrossRef]

21. An, H.J.; Kim, M.S.; Kim, J.; Son, J.; Choi, C.H.; Park, J.M.; Kim, J. Geometric evaluation of patient-specific 3D bolus from 3D printed mold and casting method for radiation therapy. *Prog. Med. Phys.* **2019**, *30*, 32–38. [CrossRef]

22. Sprowls, C.J.; Shah, A.P.; Kelly, P.; Burch, D.R.; Mathews, R.S.; Swanick, C.W.; Meeks, S.L. Whole brain radiotherapy with hippocampal sparing using Varian HyperArc. *Med. Dosim.* **2021**, *46*, 264–268. [CrossRef] [PubMed]

23. Park, S.Y.; Choi, C.H.; Park, J.M.; Chun, M.S.; Han, J.H.; Kim, J.I. A patient-specific polylactic acid bolus made by a 3D printer for breast cancer radiation therapy. *PLoS ONE* **2016**, *11*, e0168063. [CrossRef] [PubMed]

24. Park, K.; Park, S.; Jeon, M.J.; Choi, J.; Kim, J.W.; Cho, Y.J.; Jang, W.S.; Keum, Y.S.; Lee, I.J. Clinical application of 3D-printed-step-bolus in post-total mastectomy electron conformal therapy. *Oncotarget* **2017**, *8*, 25660–25668. [CrossRef] [PubMed]